AMERICAN SOCIETY FOR MICROBIOLOGY | mBio®

RESEARCH ARTICLE

Neisseria meningitidis Uses Sibling Small Regulatory RNAs To Switch from Cataplerotic to Anaplerotic Metabolism

Yvonne Pannekoek,[a] Robert A. G. Huis in 't Veld,[a] Kim Schipper,[a] Sandra Bovenkerk,[a] Gertjan Kramer,[b]* Matthijs C. Brouwer,[c] Diederik van de Beek,[c] Dave Speijer,[b] Arie van der Ende[a]

Department of Medical Microbiology, Center for Infection and Immunity (CINIMA), Academic Medical Center, Amsterdam, The Netherlands[a]; Department of Medical Biochemistry, Academic Medical Center, Amsterdam, The Netherlands[b]; Department of Neurology, Amsterdam Neuroscience, Academic Medical Center, Amsterdam, The Netherlands[c]

ABSTRACT *Neisseria meningitidis* (the meningococcus) is primarily a commensal of the human oropharynx that sporadically causes septicemia and meningitis. Meningococci adapt to diverse local host conditions differing in nutrient supply, like the nasopharynx, blood, and cerebrospinal fluid, by changing metabolism and protein repertoire. However, regulatory transcription factors and two-component systems in meningococci involved in adaptation to local nutrient variations are limited. We identified novel sibling small regulatory RNAs (*Neisseria* metabolic switch regulators [NmsRs]) regulating switches between cataplerotic and anaplerotic metabolism in this pathogen. Overexpression of NmsRs was tolerated in blood but not in cerebrospinal fluid. Expression of six tricarboxylic acid cycle enzymes was downregulated by direct action of NmsRs. Expression of the NmsRs themselves was under the control of the stringent response through the action of RelA. Small sibling regulatory RNAs of meningococci, controlling general metabolic switches, add an exciting twist to their versatile repertoire in bacterial pathogens.

IMPORTANCE Regulatory small RNAs (sRNAs) of pathogens are coming to be recognized as highly important components of riboregulatory networks, involved in the control of essential cellular processes. They play a prominent role in adaptation to physiological changes as represented by different host environments. They can function as posttranscriptional regulators of gene expression to orchestrate metabolic adaptation to nutrient stresses. Here, we identified highly conserved sibling sRNAs in *Neisseria meningitidis* which are functionally involved in the regulation of gene expression of components of the tricarboxylic acid cycle. These novel sibling sRNAs that function by antisense mechanisms extend the so-called stringent response which connects metabolic status to colonization and possibly virulence as well as pathogenesis in meningococci.

KEYWORDS *Neisseria meningitidis*, metabolic regulation, pathogenesis, sibling sRNAs, small regulatory RNAs, stringent response

Received 19 December 2016 **Accepted** 15 February 2017 **Published** 21 March 2017

Citation Pannekoek Y, Huis in 't Veld RAG, Schipper K, Bovenkerk S, Kramer G, Brouwer MC, van de Beek D, Speijer D, van der Ende A. 2017. *Neisseria meningitidis* uses sibling small regulatory RNAs to switch from cataplerotic to anaplerotic metabolism. mBio 8:e02293-16. https://doi.org/10.1128/mBio.02293-16.

Editor Julian Parkhill, The Sanger Institute

Address correspondence to Yvonne Pannekoek, y.pannekoek@amc.uva.nl.

* Present address: Gertjan Kramer, Genome Biology Unit, EMBL Heidelberg, Heidelberg, Germany.

Neisseria meningitidis causes meningitis and septicemia with a high case fatality ratio (1) but normally resides innocuously in the nasopharynx of humans. To cause disease, the meningococcus has to pass the nasopharyngeal epithelium, enter the bloodstream to cause sepsis, and subsequently cross the blood-brain barrier to cause meningitis. The different compartments encountered can be regarded as separate environments with different nutrient supplies requiring adaptation of the meningococcal metabolism (2). The bacterial reorganization of cellular transcription (and thus gene expression) upon environmental changes, such as starvation and hypoxia, is

referred to as the stringent response (3, 4). This response is mediated by the alarmones guanosine 5′,3′-bispyrophosphate and guanosine pentaphosphate, ppGpp and pppGpp, collectively referred to here as (p)ppGpp (5). In *Escherichia coli*, (p)ppGpp is synthesized from GTP and ATP via the action of two paralogous enzymes, RelA and SpoT (4, 6). The transcriptional changes occur mainly as a result of the direct effects of (p)ppGpp and its cofactor, the (protein) transcription factor DksA, on RNA polymerase (4). In addition to (p)ppGpp and regulatory proteins, among which are the transcription factors (TFs) small regulatory RNAs (sRNAs) are also involved in the switch from nutrient-rich (feast) to nutrient-limiting (famine) growth conditions of bacteria (7, 8).

sRNAs are important players in many cellular processes and prominent in those involving adaptive physiological changes. They can function as posttranscriptional regulators of gene expression to orchestrate stress responses and metabolism. Many sRNAs are synthesized upon nutritional stresses encountered by pathogens. They often regulate expression of target mRNAs that form part of a single nutritional regulatory circuit or network. sRNAs usually act by occupying or freeing up ribosomal entry sites of target transcripts as well as by regulating the accessibility of transcripts for RNases in an antisense fashion (9–12). The RNA chaperonin protein Hfq is frequently involved, enhancing these processes (13, 14).

We identified two highly conserved sRNAs, designated sibling *Neisseria* metabolic switch regulators (NmsRs), in *N. meningitidis* which are functionally involved in the regulation of tricarboxylic acid (TCA) cycle activity by antisense mechanisms. These novel sibling sRNAs extend the stringent response in meningococci, thereby connecting metabolic status to colonization and, possibly, virulence.

RESULTS

In whole-transcriptome analysis (WTA) of meningococci grown in nutrient-rich culture medium, we identified two structurally nearly identical sRNAs with 70% sequence identity (sibling sRNAs; $NmsR_A$ and $NmsR_B$), tandemly arranged in *N. meningitidis* strain H44/76 (Fig. 1) (15). Sequence read coverage of the $NmsR_B$ transcript is 5-fold (~7,500 reads/nucleotide [nt]) that of $NmsR_A$ (~1,500 reads/nt) (Fig. 1B). Among 7,335 isolates, 16 $NmsR_A$ alleles with 14 single nucleotide polymorphisms (SNPs) were observed, with 97% of the isolates sharing two alleles with only one SNP. In addition, 19 $NmsR_B$ alleles with 17 SNPs were observed, with 94% of the isolates sharing two alleles with only 4 SNPs (assessed at http://pubmlst.org/neisseria/) (16), and were located in the intergenic region in the reference *N. meningitidis* MC58 genome between locus NMB1649 (*dsbB*), encoding disulfide bond formation protein B, and NMB1650 (*lrp*), encoding leucine-responsive regulatory protein (17) (Fig. 1).

$NmsR_A$ and $NmsR_B$ overexpression impairs growth in CSF but not in blood. To investigate the functionality of NmsRs in meningococci, we created an $nmsR_A$- and $nmsR_B$-knockout strain of H44/76 (the Δ$nmsR_A$ Δ$nmsR_B$ strain) by replacing $nmsR_A$ and $nmsR_B$ with an erythromycin (Erm) resistance cassette, and we introduced a plasmid harboring the genes encoding both NmsRs, $NmsR_A$, or $NmsR_B$ into the Δ$nmsR_A$ Δ$nmsR_B$ strain, thereby generating four variant meningococcal strains, one without the NmsRs and three variants overexpressing either $NmsR_A$, $NmsR_B$, or both in isogenic backgrounds. The effect of $NmsR_A$ and $NmsR_B$ expression was first assessed in meningococci grown under two culture conditions, tryptic soy broth (TSB) (nutrient rich) and Jyssum medium (glucose as the sole carbon source [18]). All four meningococcal variants and the wild-type (wt) strain replicated equally well in rich medium (GC or TSB) (not shown). The meningococcal strain overexpressing both NmsRs did not replicate in nutrient-poor Jyssum medium, while the wt strain, Δ$nmsR_A$ Δ$nmsR_B$, and the strains harboring only single *nmsR* plasmids grew normally (Fig. 2). *In vivo* relevance of NmsRs was shown by meningococcal culture in human blood or cerebrospinal fluid (CSF). Wild-type meningococci and meningococci overexpressing NmsRs showed similar growth in blood (Fig. 2). Meningococci overexpressing NmsRs showed no growth in CSF, in contrast with wt meningococci (Fig. 2). After prolonged incubation in CSF, meningococci overex-

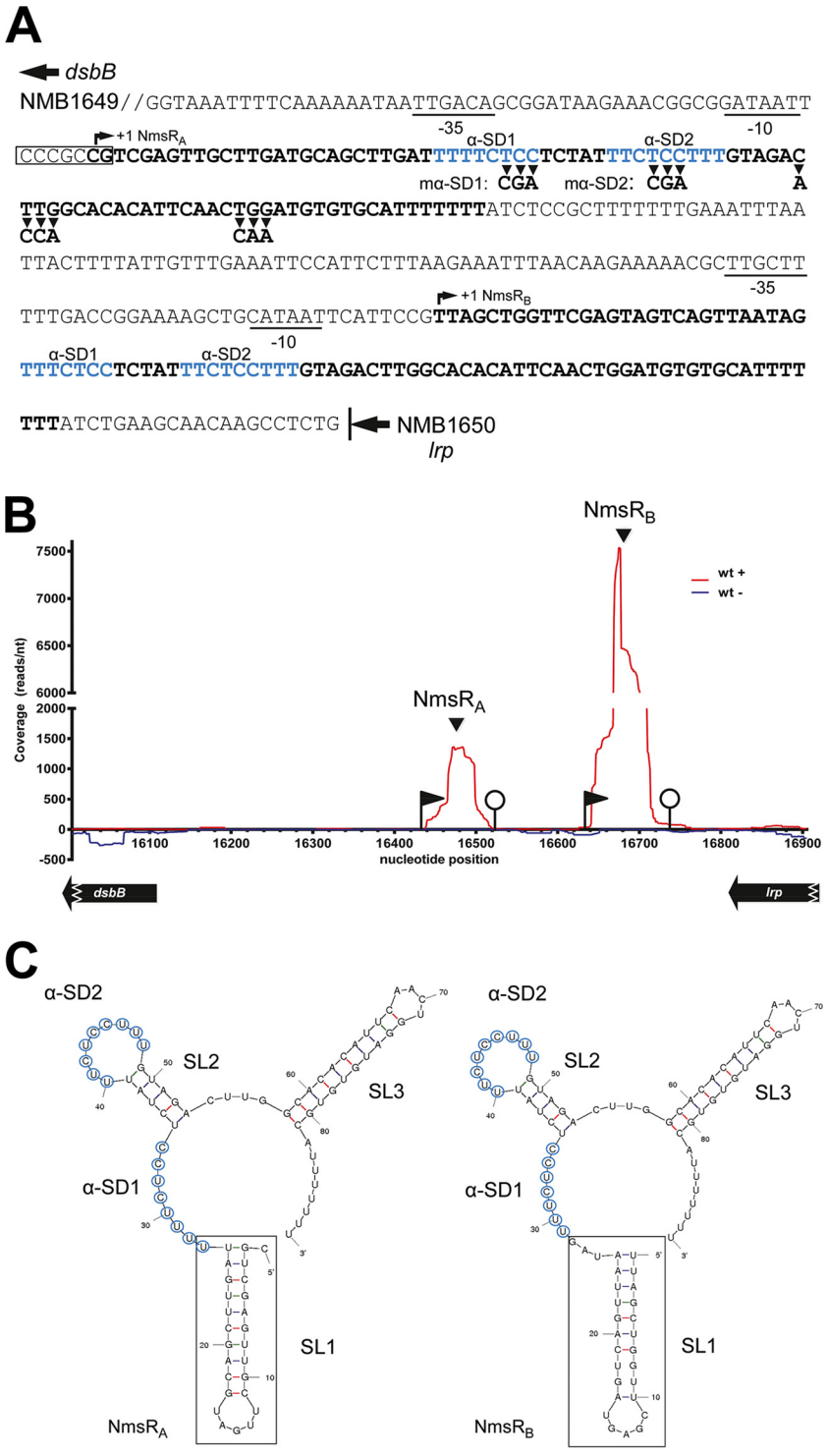

FIG 1 Primary sequence, expression analysis, and predicted secondary structures of NmsRs. (A) Sequence and genomic localization of $NmsR_A$ and $NmsR_B$ genes in *Neisseria meningitidis*. Transcriptional starts (TSSs) of $NmsR_A$ and $NmsR_B$, as determined by WTA, are indicated by +1. Putative promoter sequences (−35 and −10 boxes) are underlined. The GC-rich region between the −10 box and the TSS of $NmsR_A$ is boxed. Transcribed regions are indicated in bold. Predicted anti-Shine-Dalgarno (SD) sequence motifs (α-SD1 and α-SD2) are shown in blue; nucleotide substitutions in α-SD1 (mα-SD1) ($TCC^{32-34}\rightarrow CGA^{32-34}$) and α-SD2 (mα-SD2) ($TCC^{43-45}\rightarrow CGA^{43-45}$) of $NmsR_A$ and outside α-SD regions ($CTTG^{54-57}\rightarrow ACCA^{54-57}$ and $TGG^{71-73}\rightarrow CAA$) are indicated by arrowheads. (B) Read coverage visualization of the expression of $NmsR_A$ and $NmsR_B$ in H44/76. Transcription on the plus strand is visualized on the positive *x* axis in red; transcription on the minus strand is visualized on the negative *x* axis in blue. Nucleotide position refers to contig 28 of H44/76 WGS (AEQZ01000018.1). The black flags indicates TSSs;

(Continued on next page)

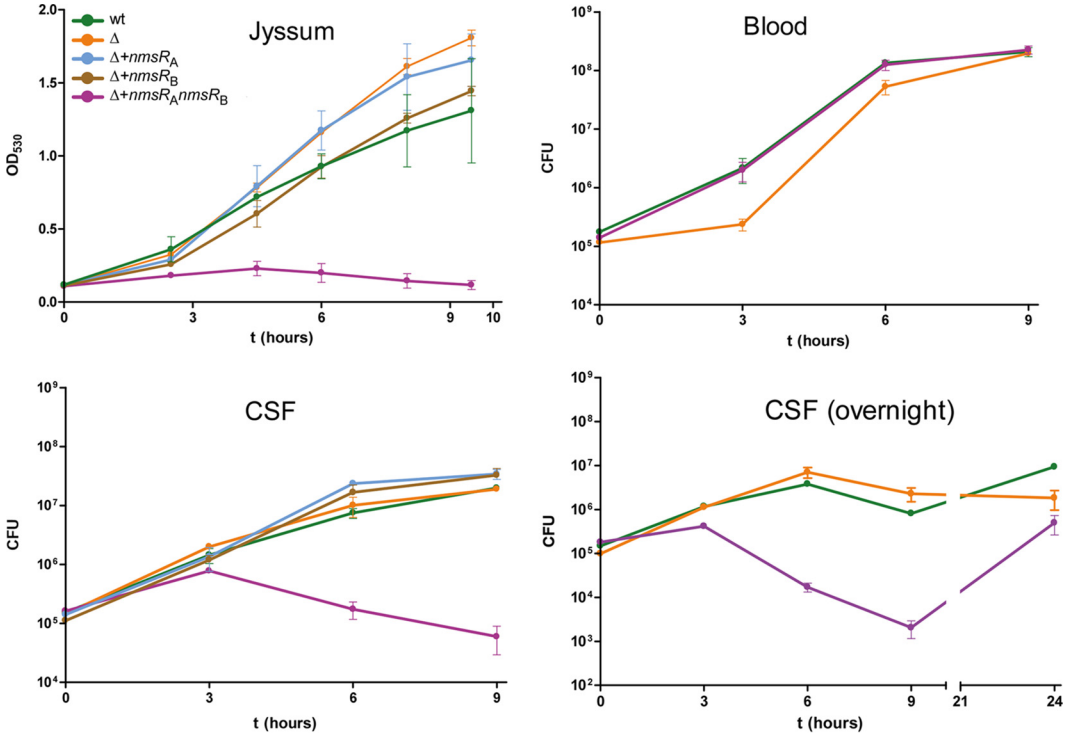

FIG 2 Overexpression of NmsRs leads to growth defects in minimal medium and CSF. Growth characteristics of different variant meningococci in Jyssum medium, blood, and CSF are shown. For growth in Jyssum medium, points represent means from two biological replicates (error bars show standard deviations); for growth curves in blood and CSF, points represent means from 5 technical replicates of one biological experiment. The different variant strains used are indicated in the figure (strain designations are explained in the legend to Fig. 4). Note that prolonged incubation (overnight) in CSF of meningococci overexpressing NmsRs results in escape variants (error bars show standard errors of the means).

pressing NmsRs did start to grow (Fig. 2). However, sequence analysis of the region encoding NmsRs showed part of $nmsR_B$ to be deleted in the escape variant.

TCA cycle enzymes of *N. meningitidis* under the control of NmsRs. To further assess the biological significance of the NmsRs, we compared the protein expression profile of the wt strain with that of the Δ$nmsR_A$ Δ$nmsR_B$ strain by mass spectrometric analysis of whole-cell lysates. Transcription of flanking genes of the Δ$nmsR_A$ Δ$nmsR_B$ strain remained unaffected after replacement of $nmsR_A$ and $nmsR_B$ with the erythromycin resistance cassette (not shown). Of all 2,300 annotated open reading frames in the *N. meningitidis* MC58 genome (17), 515 proteins (22%) were identified at the protein level. Of these, 387 yielded reliable quantification of relative expression comparing wt and Δ$nmsR_A$ Δ$nmsR_B$ strains (see Table S1 in the supplemental material). Differentially expressed proteins ranged from 7-fold upregulated to 6-fold downregulated. Using a 1.5-fold up- or downregulation as a cutoff for differential expression, a total of 18 upregulated and 10 downregulated proteins were identified (Table 1). Among the 18 proteins with increased expression in the Δ$nmsR_A$ Δ$nmsR_B$ strain, 10 (56%) were either involved in the TCA cycle directly or linked to it, such as acetate kinase (AckA-1), involved in acetyl coenzyme A (CoA) synthesis, or PrpC and PrpB, involved in propanoate metabolism feeding into the TCA cycle through succinyl-CoA. Other upregulated proteins belonged to the glycine cleavage system (GlyA), part of glycine/serine meta-

FIG 1 Legend (Continued)
the white circles indicate predicted Rho-independent terminators. Note that the region visualized encodes two distinct transcripts, indicated as $NmsR_A$ and $NmsR_B$. Coverage of the $NmsR_B$ transcript is 5-fold (~7,500 reads/nt); that of the transcripts of $NmsR_A$ is 1,500 reads/nt. (C) Predicted secondary structures of siblings $NmsR_A$ and $NmsR_B$. Secondary structures were predicted using Mfold. Unique sequences of the NmsRs are indicated by boxes. Putative α-SD sequences are circled; stem-loops are indicated as SL.

TABLE 1 Differentially (≥1.5-fold change) regulated proteins in *N. meningitidis* Δ*nmsR*$_A$ Δ*nmsR*$_B$ strain as identified by LC-MS^E

GeneID[a]	Product (gene name)[b]	Functional class (KEGG[b], String[c] and/or Uniprot[d])	wt			Δ*nmsR*$_A$*nmsR*$_B$			Δ*nmsR*$_A$ *nmsR*$_B$/wt	
			N[e]	Mean[f]	var.[g]	N[e]	Mean[f]	var.[g]	Fold[h]	*p*-value[i]
Upregulated										
NMB0434	Putative AcnD accessory protein (prpF)	TCA related[c]	0	-	-	4	0,42	13%	-	-
NMB0435	Acetate kinase 2 (ackA-1)	TCA related[d]	0	-	-	4	1,53	9%	-	-
NMB0430	Putative carboxyphosphonoenolpyruvate phosphonomutase (prpB)	Carbohydrate metabolism,TCA related[c]	0	-	-	4	0,67	18%	-	-
NMB1584	3-hydroxyacid dehydrogenase	Valine, leucine and isoleucine degradation[b] (TCA related)	1	0,23	-	4	4,74	5%	-	-
NMB1355	Aspartyl/glutamyl-tRNA amidotransferase subunit C (gatC)	Fidelity of protein synthesis[d]	1	0,83	-	4	0,65	19%	-	-
NMB0629	Phosphoribosylformimino-5-aminoimidazole carboxamide ribotide isomerase (hisA)	Histidine biosynthesis[d]	1	0,29	-	4	0,62	41%	-	-
NMB0954	Citrate synthase (gltA)	TCA[d]	4	1,86	11%	4	9,13	8%	4,9	**0,000078**
NMB1055	Serine hydroxymethyltransferase (glyA)	One-carbon metabolism[d]	4	1,46	8%	4	6,56	4%	4,5	**0,000002**
NMB0920	Isocitrate dehydrogenase NADP dependent monomeric type (icd)	TCA[d]	4	2,04	9%	4	6,57	14%	3,2	0,003223
NMB0041	ABC transporter periplasmic thiamine transport substrate-binding protein (tbpA)	Coenzyme uptake[d]	3	0,86	13%	3	2,55	4%	3,0	**0,000393**
NMB1946	ABC transporter D-methionine transport system substrate-binding protein (metQ)	D-methionine uptake[d]	4	3,18	7%	4	8,61	3%	2,7	**0,000005**
NMB0960	Succinyl CoA ligase ADP forming subunit alpha (sucD)	TCA[d]	4	4,65	7%	4	10,83	8%	2,3	**0,000422**
NMB0959	Succinyl CoA ligase ADP forming subunit beta (sucC)	TCA[d]	4	3,85	9%	4	8,70	11%	2,3	0,003188
NMB1220	Stomatin Mec 2 family protein	Possible *ftsH* regulating protein [74]	3	1,00	5%	3	2,26	8%	2,3	0,002576
NMB1572	Aconitate hydratase 2 (acnB)	TCA[d]	4	1,66	3%	4	3,58	3%	2,2	**0,000006**
NMB2096	Probable malate:quinone oxidoreductase (yojH)	TCA[d]	4	0,50	7%	4	0,98	9%	2,0	0,002223
NMB0798	ATP dependent zinc metalloprotease (ftsH)	Protease, stress response[e], cell division[b,c]	3	1,30	9%	3	2,36	6%	1,8	0,004605
NMB0431	Citrate synthase (prpC)	TCA[d]	2	1,23	6%	4	2,37	31%	1,9	0,107160

GeneID[a]	Product (gene name)[b]	Functional class (KEGG[b], String[c] and/or Uniprot[d])	wt			Δ*nmsR*$_A$*nmsR*$_B$			Δ*nmsR*$_A$*nmsR*$_B$/wt	
			N[e]	Mean[f]	var.[g]	N[e]	Mean[f]	var.[g]	Fold[h]	*p*-value[i]
Downregulated										
NMB1935	ATP synthase gamma chain (atpG)	Proton transport coupled ATP synthesis[d]	4	0,84	1%	4	0,51	13%	-1,6	0,002759
NMB1392	Glucose 6 phosphate 1 dehydrogenase (zwf)	Pentose phosphate pathway[d]	4	2,18	4%	4	1,22	6%	-1,8	**0,000173**
NMB1422	ATP dependent RNA helicase	Helicase, transcription regulation[c]	3	0,76	4%	3	0,39	12%	-2,0	0,001982
NMB1150/88	Dihydroxy acid dehydratase (ilvD1/2)	Valine, leucine and isoleucine biosynthesis[d]	4	0,59	21%	1	0,57	-	-	-
NMB0724	Phenylalanine tRNA ligase alpha subunit (pheS)	Phenylalanine tRNA loading, protein synthesis[c]	4	0,53	7%	1	0,46	-	-	-
NMB1897	Leucine tRNA ligase (leuS)	Leucine tRNA loading, protein synthesis[c]	4	0,94	19%	1	1,73	-	-	-
NMB1933	ATP synthase epsilon chain (atpC)	Proton transport coupled ATP synthesis[d]	4	0,61	20%	1	0,59	-	-	-
NMB1866	Dimethylallyl adenosine tRNA (miaB)	tRNA processing[d]	4	0,31	32%	1	0,20	-	-	-
NMB0878	Threonine dehydratase (ilvA)	Isoleucine biosynthesis, plus valine and leucine biosynthesis[b]	4	0,29	12%	1	0,24	-	-	-
NMB1084	Putative uncharacterized protein, unique to Neisseria meningitidis	Unknown	4	0,58	6%	1	0,54	-	-	-

[a]GeneID according to the work of Tettelin et al. (17).
[b]Product and protein name according to KEGG (http://www.genome.jp/kegg/).
[c]String (http://string-db.org).
[d]UniProt (http://uniprot.org/uniprot).
[e]Frequency of detection in 4 biological replicates.
[f]In normalized attomoles.
[g]Variance of standard error expressed in percent.
[h]Fold change of ≥1.5. Downregulation is expressed as the reciprocal with added "−."
[i]Independent *t* test, two-tailed, equal variable. All samples, $P \leq 0.005$ (except in red); bold values are significant after correction for false discovery rate according to the work of Benjamini and Hochberg (66). Genes indicated in green are confirmed as true targets of NmsRs in the *gfp* reporter system.

bolism, or were involved in valine, leucine, and isoleucine degradation (3-hydroxyacid dehydrogenase; NMB1584). In contrast, proteins involved in ATP synthesis-coupled proton transport (AtpG and AtpC), a protein involved in the pentose pathway (Zwf), and proteins involved in biosynthesis of valine/leucine and isoleucine (IlvD and IlvA) are downregulated without NmsRs (Table 1). Complementation of the Δ*nmsR*$_A$ Δ*nmsR*$_B$ strain with a plasmid encoding both NmsRs led to normalization of protein levels for a slight majority of the overexpressed proteins identified (10/18; results not shown). Together, these results strongly suggest that in meningococci without NmsR activity, metabolism has been switched to higher TCA cycle activities, which are less strongly coupled to respiration. As we also observed notable expression of the NmsRs in transcriptome analyses of meningococci grown in nutrient-rich medium, this implies relatively low TCA cycle activity in meningococci grown in media with abundant nutrients. In the absence of NmsRs, the role of the TCA cycle in meningococcal metabolism increases, shifting to anabolism with, e.g., breakdown products of branched-chain amino acids as anaplerotic substrates and synthesis of components beneficial for growth under nutrient-poor conditions (Table 1).

NmsR$_A$ and NmsR$_B$ translational downregulation of TCA cycle enzymes is mediated by anti-Shine-Dalgarno sequences. Results indicate that mRNAs encoding TCA cycle enzymes are potential targets for the NmsRs. *In silico* analysis (19) indeed revealed putative interactions between both NmsRs and 5′ untranslated regions (UTRs) of PrpB, PrpC, GltA, and SucC mRNAs. In addition, SdhC and FumC were identified as putative targets of NmsRs (Fig. S1 in the supplemental material). To obtain experimental evidence for the interaction between the NmsRs and potential target mRNAs, we used a well-established *gfp* reporter system in *Escherichia coli* (20). The 5′ UTR of the

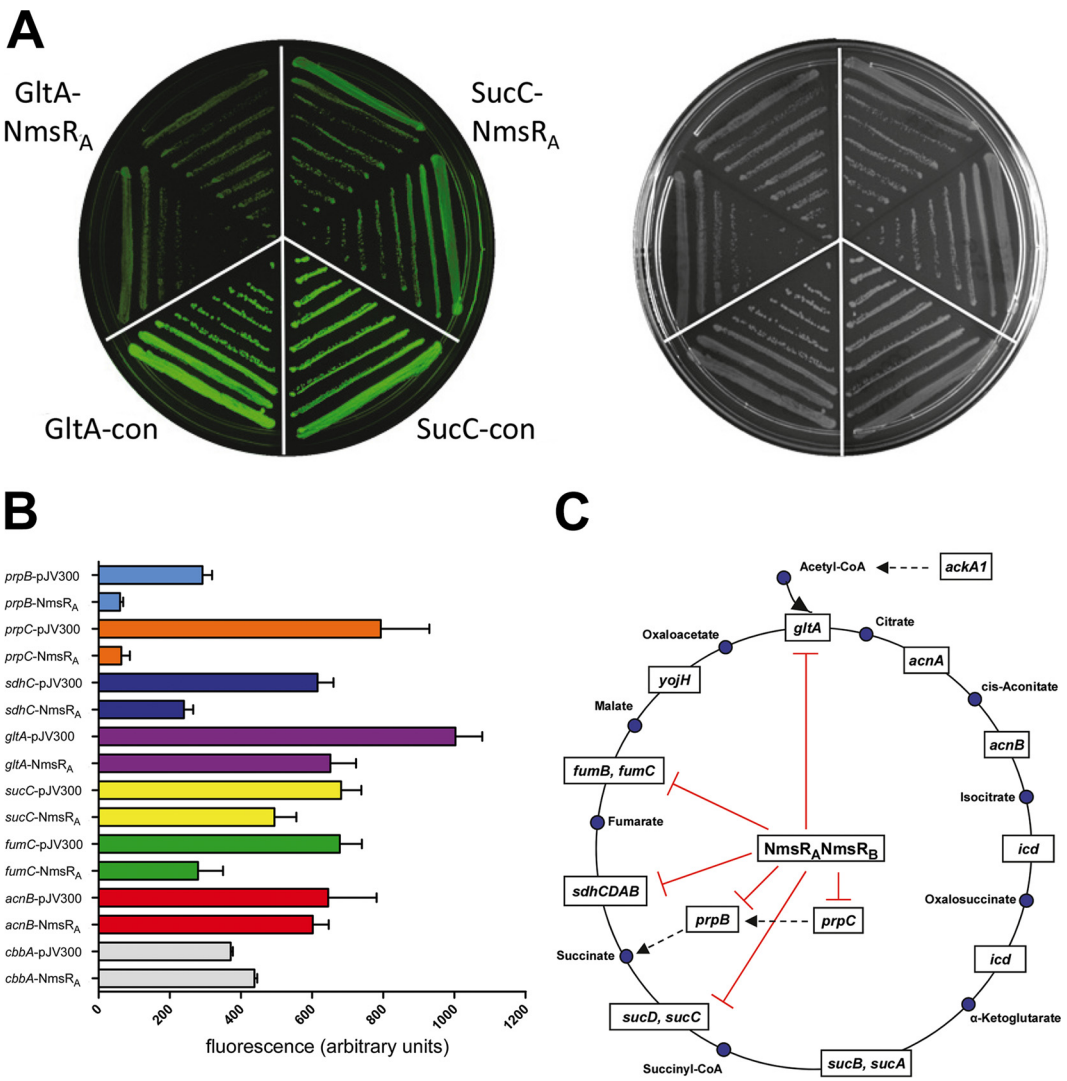

FIG 3 NmsR$_A$ regulation of target mRNA expression. (A) Repression of translational fusions *gltA*::*gfp* and *sucC*::*gfp* by NmsR$_A$. Shown are images of LB agar plates of *E. coli* carrying *gltA*::*gfp* fusion plasmid and a *sucC*::*gfp* fusion plasmid in combination with plasmid pJV300 (GltA-con and SucC-con) or pNmNmsR$_A$ (GltA-NmsR$_A$ and SucC-NmsR$_A$) obtained in the fluorescence mode (left) or the visible light mode (right). Reduced colony fluorescence of the *gltA*::*gfp* or *sucC*::*gfp* fusion strains upon NmsR$_A$ coexpression indicates regulation at posttranscriptional level. (B) **S**pecific regulation of target fusions by coexpression of NmsR$_A$. Quantification of specific fluorescence signals from cells harboring combinations of fusion plasmids pJV300 and pNmNmsR$_A$ as indicated. Error bars show standard deviations from experiments performed in quadruplicate. (C) Schematic representation of the TCA cycle with confirmed mRNA targets of NmsR$_A$. Enzymes are shown within boxes, and metabolites are shown as blue dots. Red lines (inhibitory signals) denote confirmed NmsR$_A$-downregulated target-*gfp* fusions (see text and panel B).

potential target mRNA and its first 7 to 13 codons were fused in frame to a *gfp* coding region (target-*gfp* fusion) which is constitutively expressed in *E. coli* together with the NmsRs from another plasmid vector. However, transformation of *E. coli* with plasmids harboring both *nmsR*$_A$ and *nmsR*$_B$ or only *nmsR*$_B$ failed, even when a strain (JVS-2001) was used in which the sRNA chaperonin gene *hfq* was deleted or when a low-copy-number vector was used (20). However, *E. coli* could be transformed with the plasmid harboring only *nmsR*$_A$, though it displayed attenuated growth (not shown) in all cases. Reduced fluorescence of target-*gfp* fusion in the presence of NmsR$_A$ expression, but not in the presence of expression of a control nonsense sRNA, indicates a direct interaction between NmsR$_A$ and the 5′ UTR of the target mRNA. In this way, direct translational control by NmsR$_A$ was demonstrated for six out of eight tested putative target mRNAs (*prpB*, *prpC*, *sdhC*, *gltA*, *sucC*, and *fumC* [$P < 0.005$]) (Fig. 3A and B). The observation that

fluorescence levels of the target-*gfp* fusion of two putative mRNA targets (*acnB* and *cbbA*) remained unaffected upon $NmsR_A$ expression in *trans* indicates that the slower-growth phenotype of *E. coli* upon $NmsR_A$ expression is not interfering with expression and/or proper folding of green fluorescent protein (GFP) as such (Fig. 3B).

Sequence comparison of the 5′ UTR of the target mRNAs with proven direct $NmsR_A$ interaction showed homology around the Shine-Dalgarno sequence motif (SD), part of the ribosome binding site (Fig. S1) (21). The NmsRs are predicted to fold into similar secondary structures consisting of three stem-loops (SLs) (Fig. 1C). The single-stranded region between SL1 and SL2 exposes a UC-rich sequence. This region together with the UC-rich single-stranded loop of SL2 is (partly) complementary to the SD of the target mRNAs (Fig. S1). Both of these regions, referred to as α-SDs, are completely conserved among more than 7,335 meningococcal genomes analyzed (accessed at http://pubmlst.org/neisseria/) (16). Mutagenesis of either of the α-SD sequences in $NmsR_A$ (using mutations designed to preserve the secondary structure of the NmsRs) abrogated the downregulation of all targets but GltA (Table S2). For the latter, mutagenesis of α-SD1 did not influence downregulation, but downregulation of GltA disappeared upon α-SD2 mutation (Table S2). Mutations outside α-SD regions had no effect on regulation (not shown). Replacement of nucleotides in the SD regions of the target mRNAs resulted in fluorescence levels of the cells below the level of detection. Consequently, it was not possible to investigate whether downregulation could be restored by the introduction of compensatory mutations. Taken together, these results strongly argue that $NmsR_A$ inhibits synthesis by an antisense mechanism that involves direct base pairing to 5′ UTRs of six out of eight target-*gfp* fusions assessed, presumably by preventing ribosomal entry.

NmsRs alter expression of transcript levels of TCA cycle enzymes in meningococci. The effect of NmsR expression on the expression of genes of the TCA cycle targeted by $NmsR_A$ was assessed in meningococci grown under two culture conditions, TSB (nutrient rich) and Jyssum medium (glucose as the sole carbon source [18]), in which we anticipated differential expression. Transcript levels of all $NmsR_A$ targets were indeed (1.5- to 8-fold) higher in meningococci with the NmsRs deleted and grown in TSB than in wt ($P < 0.005$). In Jyssum medium, transcript levels of *prpC*, *gltA*, and *sucC* were (5- to 3-fold) higher ($P < 0.001$) in the Δ$nmsR_A$ Δ$nmsR_B$ strain than in the wt strain. Transcript levels of *prpB* and *fumC* in Δ$nmsR_A$ Δ$nmsR_B$ and wt strains were not significantly different in Jyssum medium (Fig. 4). Of note, in all cases (except *sdhC*), the transcript levels of the targets were significantly lower in meningococci overexpressing $NmsR_A$ ($P < 0.05$) or $NmsR_B$ ($P < 0.01$) (or 2-fold lower in the case of *prpB* [$P = 0.26$]) or after overexpressing both sRNAs ($P < 0.01$) in the $NmsR_A$ and $NmsR_B$ deletion strain and in all these cases (except *sdhC*) became comparable to target levels found in wt meningococci when grown in TSB (Fig. 4). Transcript levels of *sdhC* in Jyssum medium were not significantly different in the wt strain from those in the $NmsR_A$ and $NmsR_B$ deletion strain of overexpression isogenic variants (Fig. 4).

NmsRs are connected to the stringent response and controlled by RelA. In *Neisseria gonorrhoeae*, RelA is the sole producer of (p)ppGpp (22), which acts with DskA in interacting with RNA polymerase to regulate transcription. Whether a given promoter is directly controlled by (p)ppGpp and DksA is dictated by a DNA sequence motif, the so-called discriminator. Repressed targets typically contain GC-rich 7-nucleotide discriminators between the −10 box hexamer and the transcriptional start site, whereas activated promoters harbor AT-rich discriminators at this position (3). Of note, such a GC-rich nucleotide region can be identified between the putative −10 site and the transcriptional start site of $NmsR_A$ (Fig. 1A). To investigate whether NmsRs are directly controlled by the stringent response, we created a *relA*-knockout strain of H44/76 (the Δ*relA* strain) by replacing *relA* with an erythromycin resistance cassette and assessed $NmsR_A$ and $NmsR_B$ levels after growth in TSB or Jyssum medium by reverse transcription-quantitative PCR (RT-qPCR). We did not obtain viable meningococci when *relA* was expressed in *trans*. Of interest, upon deletion of *relA*, $NmsR_A$ transcript levels

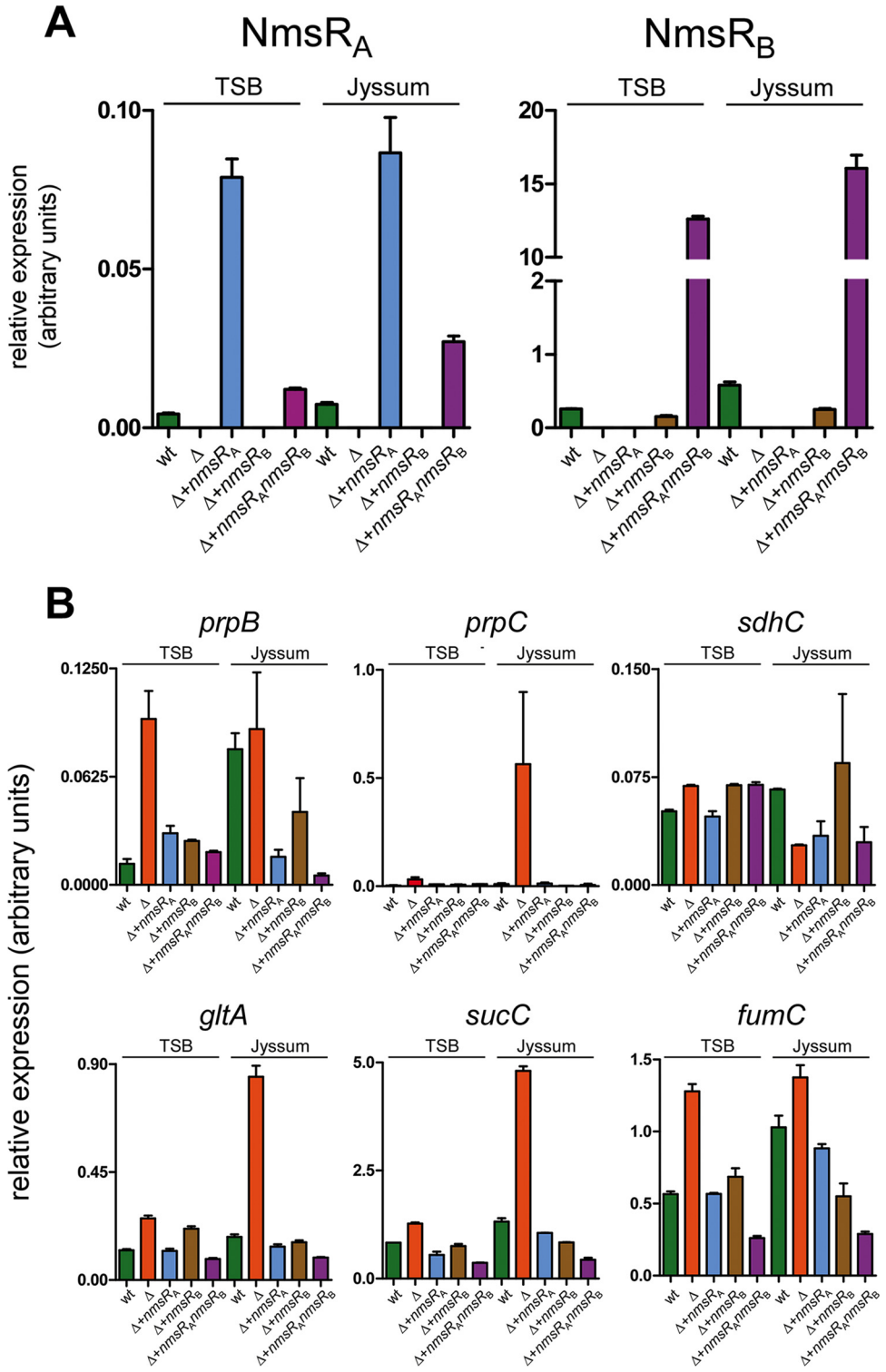

FIG 4 Transcript levels of TCA cycle enzymes in meningococci are under the control of NmsRs. (A) Relative expression levels of NmsRs. Transcript levels assessed by RT-qPCR in wt meningococci, in meningococci in which *nmsR*$_A$ and *nmsR*$_B$ are deleted (Δ) and in the Δ strain overexpressing NmsR$_A$ (Δ+*nmsR*$_A$), overexpressing NmsR$_B$ (Δ+*nmsR*$_B$), or overexpressing *nmsR*$_A$ and *nmsR*$_B$ (Δ+*nmsR*$_A$*nmsR*$_B$) (error bars, standard errors of the means; technical replicates, $n = 8$, over biological, $n = 3$). Meningococci were cultured in TSB (nutrient rich) and Jyssum medium (glucose as the sole carbon source [18]). (B) Relative expression levels of NmsR targets. Transcript levels assessed by RT-qPCR in wt meningococci and in meningococci in which *nmsR*$_A$ and *nmsR*$_B$ are deleted (Δ) and in the Δ strain overexpressing NmsR$_A$ (Δ+*nmsR*$_A$), overexpressing NmsR$_B$ (Δ+*nmsR*$_B$), and overexpressing *nmsR*$_A$ and *nmsR*$_B$ (Δ+*nmsR*$_A$*nmsR*$_B$) (error bars, standard errors of the means; technical replicates, $n = 8$, over biological, $n = 3$). Meningococci were cultured in TSB (nutrient rich) and Jyssum medium (glucose as the sole carbon source [18]).

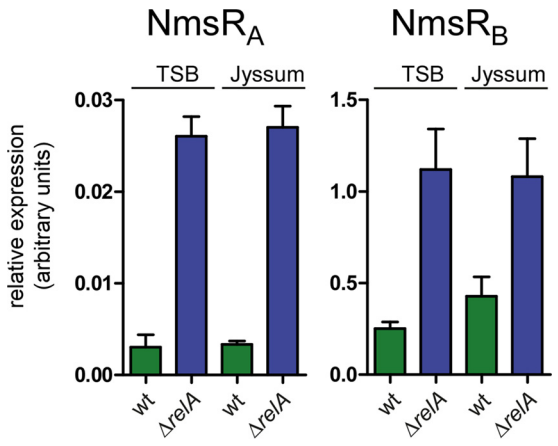

FIG 5 NmsR$_A$ and NmsR$_B$ levels in meningococci are under the control of the stringent response. Relative expression levels of NmsR$_A$ and NmsR$_B$, assessed by RT-qPCR, in wt meningococci and in meningococci in which *relA* is deleted (Δ*relA*) after growth in TSB (nutrient rich) and Jyssum medium (glucose as the sole carbon source [18]) (error bars, standard errors of the means; technical replicates, $n = 8$, over biological, $n = 3$).

were 10-fold higher than wt levels ($P < 0.0001$), reaching levels that were comparable to NmsR$_B$ levels in wt cells grown in TSB. NmsR$_B$ levels were also significantly higher in Δ*relA* cells and increased 5- ($P < 0.0005$) and 2.5-fold ($P < 0.05$) in TSB and Jyssum medium, respectively (Fig. 5). No significant difference in levels of NmsRs was observed between cells grown in medium with glucose as sole carbon source and cells grown in nutrient-rich medium (Fig. 5).

We next investigated whether transcript levels of the NmsR$_A$ targets were affected upon deletion of *relA*. Transcript levels of all NmsR$_A$ targets except *sdhC* in cells grown in TSB were relatively low and comparable in wt and Δ*relA* cells. In Jyssum medium, the transcript levels of all targets in the wt strain, again with the exception of *sdhC*, were 2- to 17-fold higher ($P < 0.0005$) than levels in cells cultured in TSB (Fig. 6). However, upon deletion of *relA*, transcript levels of *prpB*, *prpC*, *gltA*, and *sucC* were inversely correlated with levels of NmsR$_A$ and NmsR$_B$. In Jyssum medium, the transcript levels of the targets in Δ*relA* meningococci were 2- to 7-fold lower ($P < 0.0001$) than in wt meningococci and comparable to levels in wt cells or Δ*relA* cells grown in TSB (Fig. 6). Upon deletion of *nmsR*$_A$ and *nmsR*$_B$ in the Δ*relA* strain (Δ*relA* Δ*nmsR*$_A$ Δ*nmsR*$_B$) in cells cultured in TSB, the transcript levels of all targets, with the exception of *sdhC*, were 2- to 10-fold higher than those in Δ*relA* and wt strains. Of note, transcript levels of *prpB*, *prpC*, *gltA*, and *sucC* in the triple mutant Δ*relA* Δ*nmsR*$_A$ Δ*nmsR*$_B$ cells grown in Jyssum medium were 2- to 5-fold higher ($P < 0.0001$) than in the single Δ*relA* mutant. These results confirmed *relA*-mediated downregulation of NmsRs, irrespective of the culture conditions used. Transcript levels of *sdhC* and *fumC* in the triple-knockout Δ*relA* Δ*nmsR*$_A$ Δ*nmsR*$_B$ strain remained unaffected in Jyssum medium compared to the Δ*relA* single knockout (Fig. 6).

DISCUSSION

In this study, we identified novel sibling regulatory sRNAs of *N. meningitidis* that establish a connection between the stringent response and the riboregulatory network. Our data showed regulation of the TCA cycle activity by direct action of sibling sRNAs in *N. meningitidis*. The expression of NmsRs themselves is under the control of the stringent response via RelA. The activity of the sibling sRNAs is crucial when meningococci encounter different host environments with variable nutrient supplies, such as blood and CSF. High sibling sRNA expression allows replication and survival in blood but impairs growth in CSF. Whether this is solely due to differential expression of TCA cycle enzymes or whether other, so-far-unknown targets are involved is the subject of further study.

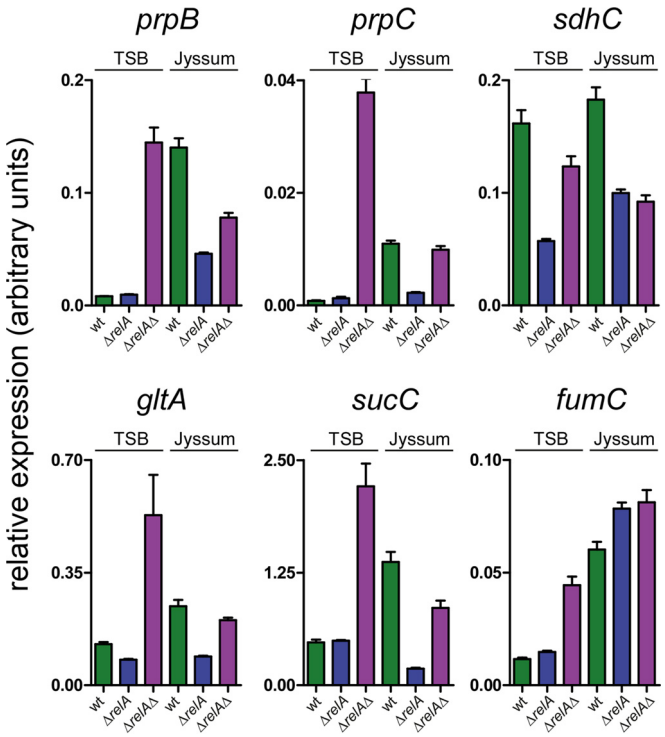

FIG 6 Transcript levels of NmsR targets are under the control of the stringent response by *relA*. Relative expression levels of NmsR targets, assessed by RT-qPCR, in wt meningococci, in meningococci in which *relA* is deleted (Δ*relA*), and in meningococci in which *relA* $nmsR_A$, and $nmsR_B$ are deleted (Δ*relA*Δ) after growth in TSB (nutrient rich) and Jyssum medium (glucose as the sole carbon source [18]) (error bars, standard errors of the means; technical replicates, $n = 5$, over biological, $n = 1$).

NmsRs are the first sibling sRNAs and only the third sRNA species in *Neisseria* for which target genes are experimentally confirmed (23). NrrF, a Fur-regulated sRNA, has been identified in meningococci (24, 25) and gonococci (26) and is upregulated under iron-depleted conditions. This sRNA has been shown to be involved in regulation of *sdhA*, belonging to the operon encoding the succinate dehydrogenase complex (*sdhCDAB*). Recently, an sRNA was identified in *N. gonorrhoeae* that acts in *cis* and influences antigenic variation of pilin (27). Other sRNAs, among them AniS in meningococci and FnrS in gonococci, are synthesized under oxygen limitation, but their targets remain elusive (28, 29). The same is true for a σ^E-dependent sRNA that has been identified in *N. meningitidis* (15).

By employing proteomics, putative targets of the NmsRs were identified. We experimentally validated direct interaction for four mRNAs coding for enzymes belonging to the TCA cycle (*sdhC*, *gltA*, *sucC*, and *fumC*) and for two mRNAs encoding enzymes producing intermediates of the TCA cycle (*prpB* and *prpC*) (schematically represented in Fig. 3C). Of interest was our identification of *sdhC* as a direct target of NmsRs. *sdhC* is the first gene of the cluster *sdhCDAB*, coding for the succinate dehydrogenase complex. This complex, which generates fumarate from succinate during the TCA cycle, concomitantly feeds electrons to the respiration chain (30). As mentioned before, in meningococci, NrrF has been shown to be involved in the Fur-dependent regulation of genes belonging to this cluster (24, 25). Although we showed a direct interaction between $NmsR_A$ and *sdhC* resulting in downregulation of GFP by using the *gfp* reporter system, in the genetic background of meningococci we did not observe regulation. Likewise, we were also not able to confirm regulation for FumC in meningococci. This might imply either that both mRNAs are not true targets of $NmsR_A$ or that expression of these transcripts, in the genetic background of meningococci, is more complex, e.g., under the control of other regulators as well. The latter is not unlikely since it has been shown that transcript levels of *sdhC* are controlled by the two-component regulator MisR (31),

and as mentioned above, *sdhA* levels are controlled by NrrF. If true, *sdhCDAB* might be the first example of a cistronic mRNA in meningococci that is subject to regulation by two different sRNA species as well as a two-component regulator.

We identified *prpB* and *prpC* as targets of NmsRs. It has been shown that expression of these genes enables survival of the meningococci in the "normal" habitat (i.e., the adult nasopharynx) by allowing utilization of propionic acid as a supplementary carbon source (32). Thus, use of propionate becomes crucial under conditions of nutrient limitation. These observations are nicely in line with our data, as overexpression of NmsRs under nutrient-limiting conditions (e.g., Jyssum medium or liquor) leads to growth arrest. Tightly regulating NmsR expression is an essential prerequisite to support growth under divergent *in vivo* conditions, exemplified by colonization of the nasopharynx and replication in CSF.

We convincingly demonstrated that the expression of at least four different mRNA species is controlled by NmsRs. This makes NmsRs, as far as we know, the first example of sibling sRNAs in *N. meningitidis* acting on multiple *trans*-encoded targets, thus rewiring interconnected transcriptional networks, possibly including the MisR and Fur regulon. The unexpected transcript levels of *sdhC* and *fumC* observed with some strain-growth condition combinations could reflect such complex regulation.

Many small RNAs are known to contain one single-stranded domain that is able to interact with multiple target mRNAs (33–37). Other sRNAs have several functional domains that base pair with different sets of target mRNAs (38–41). Using *in vivo* experiments, we demonstrated that $NmsR_A$ represses synthesis of its mRNA targets most likely by an antisense mechanism. This involves base pairing of predicted single-stranded α-SD regions (UC-rich) of the NmsRs to a sequence stretch overlapping the SD in the targets. Basically, this antisense mechanism is shared by many other sRNAs (7, 42). Of interest, the NmsRs contain two α-SD regions apparently acting on the same set of mRNAs by duplex formation with the region encompassing the SD. Both α-SD regions are characterized by UC-rich stretches but differ slightly from each other in sequence. In five out of six cases, action of both α-SDs is required for downregulation, suggesting coordinated activity, while in one case (*gltA*) downregulation is abrogated only after mutating α-SD2. This suggests that, for this target, α-SD2 acts independently of α-SD1 and that only duplex formation with α-SD2 is essential. Calculation of the minimum free energy (MFE) of the duplexes before and after mutagenesis of the α-SDs using *RNAhybrid* (43) could not accurately predict the *in vivo* outcome of this regulation (not shown). However, similar modes of action have recently been described for the LhrC family of sibling sRNAs of *Listeria monocytogenes* (44, 45), and future experiments are necessary to investigate whether, for example, less conserved flanking sequences of the region of interaction of NmsRs with their targets might contribute to a different affinity and subsequent outcome of the duplex formation. The finding that *in silico* predictions of duplex formation based on complementarity of target and sRNA sequences do not always match *in vitro* observations, e.g., the predicted target *cbbA* apparently not being controlled by $NmsR_A$, is also important in this context.

We observed that expression of both NmsRs or $NmsR_B$ in *E. coli* did not result in viable cells, while expression of $NmsR_A$ in *E. coli* showed attenuated growth. Possibly, the expression of both NmsRs is toxic for *E. coli*. Alternatively, *E. coli* encodes (an) $NmsR_A$ and $NmsR_B$ target(s), which will be interesting to identify as well. This interpretation is strengthened by the observation that the slower-growth phenotype of *E. coli* disappeared after mutagenesis of the α-SDs of $NmsR_A$ (not shown).

The activity of many sRNAs in bacterial pathogens depends on the RNA chaperone Hfq (13, 14, 46). Among the direct targets of $NmsR_A$ identified, three proteins (GltA, PrpB, and PrpC) were also found to be overexpressed in an Hfq deletion strain of *N. meningitidis* (Δhfq) (47). This overlap between some of the $NmsR_A$ targets and Hfq-dependent mRNAs might indicate that for these cases NmsRs act in concert with Hfq. In general, two signatures in the sequences of sRNAs are reported as preferred binding sites for Hfq. The first is a typical A/U-rich single-stranded stretch that precedes the predicted Rho-independent terminator. The second signature consists of terminal U

residues (14, 48, 49). The second signature is obviously present, but the first signature seems absent from NmsRs. Thus, whether the observed overlap between the Hfq and $NmsR_A$ regulon in *N. meningitidis* represents a joint action of the chaperone and sRNAs, or represents a more indirect phenomenon, awaits further experiments.

The continuous discovery of more sRNAs has resulted in the identification of several examples of homologous sRNAs, "sibling" sRNAs (50). We identified a novel sibling member of this expanding class of sRNAs. The NmsRs are encoded in tandem in an intergenic region. Equal expression levels of the two sRNAs were observed under nutrient-rich and nutrient-poor conditions, but relative expression levels of $NmsR_A$ were very low compared to those of $NmsR_B$. The relatively high expression levels of $NmsR_B$ might suggest that $NmsR_B$ acts redundantly in a compensatory manner on the same targets, as has been described for sRNAs of other pathogens (36, 51, 52). The system is more complicated, however, as illustrated by the fact that target levels were significantly downregulated upon overexpression of single NmsRs but expression of both was required for complete repression (demonstrating combined NmsR action). In addition, the action of both sRNAs was also required for growth inhibition of meningococci under nutrient-limiting conditions. Thus, these observations suggest classification of NmsRs as riboregulators that act cumulatively, each contributing in a different degree to overall adaptation. Homologous sRNAs acting together have also been described for other pathogens (50, 53). It should be noted that although single $NmsR_A$ levels were low and single $NmsR_B$ levels were significantly lower when they were expressed in $\Delta nmsR_A$ $\Delta nmsR_B$ cells, they were still sufficient to downregulate 5′ UTR *gfp* fusion products in *E. coli* and mRNA target levels in meningococci.

How the meningococcal NmsRs are regulated themselves and whether they are fine-tuned individually with regard to their own expression levels as well as their target preferences have to be elucidated further. We could show the expression of NmsRs to be elevated in a *relA* knockout, indicating that it is connected to the stringent response. A direct interaction of (p)ppGpp with the putative negative discriminator in the 5′ UTR of $NmsR_A$ looks tempting. Of interest, many gammaproteobacterial genes shown to be direct targets of (p)ppGpp contain typical σ^{70}-dependent promoters (3). Indeed, inspection of the predicted promoter region of $NmsR_A$ shows a high similarity to σ-dependent promoters with the σ^{70} signatures identified in *E. coli* (−35 element TTGACA [*E. coli* consensus TTGACA] and −10 element GATAAT [*E. coli* consensus TATAAT]) (54–56). Also, the 5′ UTR of $NmsR_B$ has an, albeit weaker, σ^{70} signature. This might suggest σ-dependent $NmsR_A$ transcription directly controlled by (p)ppGpp. Expression levels of $NmsR_B$ are much higher when the two single sRNAs are coexpressed, reflecting less restricted transcription for this sRNA. Cotranscription of the two sRNAs might also be needed for their stabilization. How the possible mutual stabilization and interregulation might work is under investigation. Alternatively, the NmsRs are indirectly controlled by (p)ppGpp. In some cases, regulators of sRNA expression are located in the close vicinity of the particular sRNA to be regulated (57). The gene encoding Lrp (NMB1650) is located directly downstream of the locus encoding the sibling sRNAs (though in opposite orientation). The expression of Lrp might be stimulated by (p)ppGpp (58). However, NmsR levels did not significantly change upon either deletion or overexpression of *lrp* (not shown).

In conclusion, we identified sibling sRNAs targeting genes encoding TCA cycle enzymes, stressing their importance in the adaptation to changing environments in the host. The riboregulated network of the sibling sRNAs is part of the RelA-regulated stringent response. NmsRs of *N. meningitidis* form a crucial part of the riboregulatory network monitoring metabolic status, translating this into colonization with likely implications for pathogenesis.

MATERIALS AND METHODS

Bacterial strains and culture conditions. *N. meningitidis* strain H44/76, B:P1.7,16: F3-3:ST-32 (cc32), is closely related to the sequenced serogroup B strain MC58, belonging to the same clonal complex (59). Meningococci were grown for 16 to 18 h on GC plates (Difco) supplemented with 1% (vol/vol) Vitox (Oxoid) or on PVX plates (bioMérieux) at 37°C in a humidified atmosphere of 5% CO_2. Broth culturing was

performed in tryptic soy broth (TSB) (BD), GC medium supplemented with 1% (vol/vol) Vitox, or Jyssum medium (18), on a gyratory shaker (180 rpm) at 37°C. When appropriate, plates or broths were supplemented with erythromycin (Erm) (5 μg/ml) and/or chloramphenicol (Cm) (5 μg/ml) and/or kanamycin (50 μg/ml). Expression of recombinant DNA in meningococci was induced by IPTG (isopropyl-β-D-thiogalactopyranoside) (0.5 mM). Growth in broth was monitored by measuring optical density of cultures at 530 nm (OD_{530}) at regular time intervals. Growth of meningococci in human blood and CSF was monitored as follows. Blood was collected in 4-ml Vacutainers with 17 IU/ml sodium heparin (BD) from a healthy male volunteer approximately 2 h prior to use. CSF was extracted, with informed consent, from patients with suspected normal-pressure hydrocephalus, either used fresh (within $<$24 h stored at 4°C) or aliquoted and stored at $-$80°C. CSF white blood cell count and glucose and protein levels were within normal range. Heparinized human blood and CSF, the latter diluted prior to use to 50% (vol/vol) with phosphate-buffered saline (PBS), was inoculated with the equivalent of approximately 1×10^5 meningococci, which were obtained from precultures in TSB (OD_{530}, ~0.2 to 0.4). Aliquots of 220 μl were incubated in sterile 96-well plates (Corning) and incubated at 37°C in a humidified atmosphere of 5% CO_2. At regular time intervals, 20-μl samples were serially diluted and plated on PVX plates (bioMérieux), and colonies were counted after 16 to 18 h of growth at 37°C in a humidified atmosphere of 5% CO_2.

E. coli strain Top10 (Invitrogen) was used to clone *gfp* fusions and in experiments involving coexpression of *gfp* fusions and sRNAs. *E. coli* strain Top10F′ (Invitrogen) was used to clone sRNA expression plasmids and pCR2.1 (Invitrogen) and pEN11-*pldA* (60) constructs. *E. coli hfq*-knockout strain JVS-2001 was kindly provided by J. Vogel (Würzburg, Germany). *E. coli* strains were grown in lysogeny broth (LB) (Oxoid) (2% [wt/vol] in distilled water [dH_2O]) or on LB agar (1% [wt/vol]) plates. Liquid *E. coli* cultures were grown in 5 ml of medium inoculated from a single colony overnight at 37°C on a gyratory shaker (250 rpm). Antibiotics were applied to *E. coli* cultures at concentrations of 100 μg/ml (ampicillin) and 20 μg/ml (chloramphenicol).

Plasmid DNA from *E. coli* was isolated from overnight cultures grown in LB using the Wizard Plus SV Minipreps DNA kit (Promega). PCRs were performed according to standard protocols using a Biometra PCR machine. Primer sequences are listed in Table S3 in the supplemental material. DNA was gel purified using a GeneJET gel extraction kit (Thermo Scientific). Digestion and ligation were carried out using enzymes supplied by New England BioLabs or Thermo Scientific. Plasmid pCR2.1 was used for cloning and sequencing of PCR products. Plasmids pXG-0 (control for autofluorescence), pXG-1 (control for sRNA effect on *gfp* expression), and pXG-10 (standard plasmid for *gfp* fusion cloning) were kindly provided by J. Vogel (Würzburg, Germany) and have been described previously (20). The $nmsR_A$ gene was amplified using primers RHsRNA25CFW11 and RHsRNA25GFPRV13b and inserted into the sRNA-expressing plasmid pZE12-*luc*, thereby creating pNmNmsR$_A$ using the cloning strategy described previously (20). The shuttle vector pEN11-*pldA* was used to express sRNAs in meningococci (60).

N. meningitidis was transformed as described previously (61). Transformants were plated on selective plates containing appropriate antibiotics and checked by PCR for integration and orientation of the erythromycin or kanamycin resistance cassette. All constructs were verified by Sanger sequencing.

Fluorescence measurements of *gfp E. coli* reporter strains and data processing. *E. coli* Top10 cells expressing *gfp* fusions were streaked on standard LB plates supplemented with appropriate antibiotics. After overnight growth, colonies were photographed in a Syngene Bio Image analyzer using a Lumenera camera with a 510-nm emission filter and excitation at 460 nm. Fluorescence measurements in 96-well plates were carried out as described previously (20). In brief, single colonies (in quadruplicate) of *E. coli* strains harboring a target-*gfp* fusion and sRNA-expressing plasmids were inoculated in 200 μl LB in a 96-well microtiter plate, and cultures were grown at 37°C. The OD was measured at 600 nm in an enzyme-linked immunosorbent assay (ELISA) reader (Anthos Labtec), and fluorescence was measured (optical excitation filter, 485/20 nm; emission filter, 530/25 nm) in a CytoFluor II multiwell plate reader (PerSeptive Biosystems). The linear range of increasing fluorescence during growth covered by all members of a quadruplicate was selected to obtain the specific fluorescence. To calculate the specific fluorescence, the total fluorescence of a given strain expressing NmsR$_A$ and a target-*gfp* fusion gene (the mean fluorescence of the quadruplicate at a chosen time point within the linear range) was corrected for the autofluorescence measured in strains harboring an NmsR$_A$ expression plasmid or control sRNA in combination with the negative-control plasmid pXG-0 (expressing luciferase, i.e., no *gfp*). The regulatory effect of NmsR$_A$ on a target-*gfp* fusion was expressed as fold regulation (mean of the quadruplicate values). This is calculated by dividing the unregulated *gfp* fusion specific fluorescence (negative-control sRNA pJV300) by the regulated *gfp* fusion specific fluorescence (sRNA of interest) (20).

Construction of Δ$nmsR_A$ Δ$nmsR_B$ and Δ*relA* mutants of *N. meningitidis* strain H44/76. *N. meningitidis* H44/76 knockout mutants of $nmsR_A$ and $nmsR_B$ and of *relA* (NMB1735) were constructed using the PCR-ligation-PCR method as described previously (62). PCR products were generated with primer pairs YPsRNA25FWKO1-YPsRNA25RPKO2 and YPsRNA25FWKO3-YPsRNA25RPKO4 to create the Δ$nmsR_A$ Δ$nmsR_B$ strain and primer pairs KSrelAF1-KSrelAR2 and KSrelAF6-KSrelAR7 to create the Δ*relA* strain and ligated. The ligation products were reamplified with primer pair YPsRNA25FWKO1-YPsRNA25RPKO4 (for Δ$nmsR_A$ Δ$nmsR_B$) and primer pair KSrelAF1-KSrelAR7 (for Δ*relA*). Resulting PCR products were cloned into pCR2.1 (Invitrogen). The EcoRI-digested Erm resistance cassette from pAErmC′ was introduced into the created unique MfeI restriction site, yielding plasmids pCR2.1-sibling sRNA and pCR2.1-NMB1735 (*relA*) (62). The Δ$nmsR_A$ Δ$nmsR_B$ and Δ*relA* knockout strains were generated by natural transformation of strain H44/76 with pCR2.1-NmsR$_A$NmsR$_B$ and pCR2.1-NMB1735, respectively, with selection for Erm resistance. Replacement of NmsR$_A$ and NmsR$_B$ and NMB1735 by the Erm cassette was confirmed by PCR with primer pairs that were used for amplification of the ligation products and sequence analysis. Mutant strains in which the transcriptional direction of the Erm cassette was in accordance with the original transcriptional direction of the deleted genes

were selected. To create the Δ*relA* Δ*nmsR*$_A$ Δ*nmsR*$_B$ triple-knockout strain, the same strategy as that described for the creation of single knockouts was used, but in this case, the *relA* gene in the Δ*nmsR*$_A$ Δ*nmsR*$_B$ strain was replaced by a kanamycin resistance cassette. The kanamycin resistance cassette was amplified using plasmid pDOC-F as the template and primer set pDOCF1 and pDOCF2 (63), and primer KSrelAF6-P in combination with primer KSrelAF7 was used instead of primer KSrelAF6. Transcription of flanking genes of the knockout strains was controlled by RT-qPCR and remained unaffected.

Overexpression of *nmsR*$_A$ and *nmsR*$_B$ and *relA*. The construction of plasmids overexpressing sRNAs was carried out as described previously (60). In brief, for *nmsR*$_A$ and *nmsR*$_B$ together and separately, the regions encoding both NmsR$_A$ and NmsR$_B$, only NmsR$_A$, and only NmsR$_B$ of strain H44/76 were amplified with primer pairs CT_sRNA25FW/CT_sRNA25Rev (for both NmsR$_A$ and NmsR$_B$), RHsRNA25CFW11/RHsRNA25CRV13b (for NmsR$_A$ only), and RHsRNA25CFW12/RHsRNA25CRV13b (for NmsR$_B$ only). Reverse primers contained an RcaI site. Primer pair YPpen11MauB1-YPpen11plus1, with pEN11-*pldA* as the template, was used to generate a part of pEN11-*pldA* containing a MauBI restriction at the 3′ end and the promoter sequence and the region between the −10 box and the transcriptional start of the farthest part of the 5′ end. This fragment was ligated to the PCR products encoding both NmsR$_A$ and NmsR$_B$ or NmsR$_A$ and NmsR$_B$ separately, and the ligation product was PCR amplified using primer pair YPpen11MauB1-CT_sRNA25Rev (for NmsR$_A$ and NmsR$_B$ together) and primer pair YPpen11MauBI-RHsRNA25CRV13b (for NmgR$_A$ and NmsR$_B$ separately). The resulting PCR products and pEN11-*pldA* were digested with MauBI and BspHI, ligated into MauBI- and BspHI-predigested pEN11-*pldA*, and transformed to *E. coli* Top10F′ (Invitrogen). Cm-resistant colonies were checked by colony PCR and sequencing, using pEN11FW2 and pEN11R primers. Plasmids of clones containing an intact coding region for both NmsR$_A$ and NmsR$_B$ (pEN11_NmsR$_A$NmsR$_B$) or an intact NmsR$_A$ or NmsR$_B$ (pEN11_NmsR$_A$ or pEN11_ NmsR$_B$, respectively) were isolated to transform H44/76, thereby generating H44/76+pEN11_NmsR$_A$NmsR$_B$, H44/76+pEN11_NmsR$_A$, and H44/76+pEN11_NmsR$_B$, respectively. Because transformation of cells (*E. coli* or meningococci) with constructs overexpressing *relA* did not yield viable cells, we did not succeed in creating a strain overexpressing *relA*.

***In vitro* mutagenesis of *nmsR*$_A$.** Construct pNmNmsR$_A$ was used to generate mutant sNmsR$_A$s. Point mutations were generated using QuikChange site-directed mutagenesis (Stratagene). Two mutants of pNmNmsR$_A$ in α-SD regions were generated, pNmNmsR$_A$mα-SD1 and pNmNmsR$_A$mα-SD2, using primer pair RHsR25A1eSD_F-RHsR25A1eSD_R (for mutant pNmNmsR$_A$mα-SD1) and primer pair RHsR25A2eSD_F-RHsR25A2eSD_R (for mutant pNmNmsR$_A$mα-SD2). Two mutants of pNmNmsR$_A$ outside α-SD regions were generated, pNmNmsR$_A$mLoop3 and pNmNmsR$_A$m2Loop, using primer pair YPsR25Loop3_F-YPsR25Loop3_R (for mutant pNmNmsR$_A$mLoop3) and primer pair RHsR25A2Loop_F-RHsR25A2Loop_R for pNmNmsR$_A$m2Loop). Mutations were confirmed by sequence analysis.

WTA and RT-qPCR. WTA was carried out as described previously (15). For RT-qPCR, RNA was extracted from meningococci grown to log phase (OD_{600}, 0.2 to 0. 5) using the miRNeasy minikit (Qiagen) followed by Turbo DNase Turbo DNA-free kit (Life Technologies) treatment. Then, cDNA was synthesized from 1.5 μg of RNA and random oligonucleotide hexamers using ThermoScript reverse transcriptase (RT) (Invitrogen) according to the manufacturer's recommendations. Quantitative PCR was performed using LightCycler 480 SYBR Green I Master in the LightCycler 480 system (Roche). The identities of the resulting amplicons were checked by melting-curve analysis using the LightCycler 480 and 1.5% agarose gel electrophoresis. Reaction mixtures containing no template were included in each real-time PCR experiment to control for contamination. Transcripts of target and reference genes were analyzed using LinRegPCR version 2014.2 (64). Constitutive relative gene expression in medium was determined as a ratio of target gene to reference genes (*rmpM* [NMB0382] and *cbbA* [NMB1869]).

Sample preparation and mass spectrometric analysis. Cells from mid-logarithmic-phase Δ*nmsR*$_A$ Δ*nmsR*$_B$ and wt strains were rapidly cooled and harvested by centrifugation. Cell pellets were resuspended in lysis buffer consisting of 0.1% RapiGest SF (Waters Corporation, Milford, MA) in 50 mM ammonium-hydrogen carbonate (pH 8.0) (Sigma-Aldrich) and lysed by sonication. The protein content of the different samples was determined by bicinchoninic acid assay (Thermo Scientific, Rockford, IL) using the manufacturer's protocol. Overnight proteolysis of samples and subsequent removal of RapiGest surfactant were performed according to the protocol provided with RapiGest SF for in-solution digestion using a 1:50 (wt/wt) ratio of trypsin (Promega, Madison, WI) to protein. Peptide samples were then mixed 1:1 (vol/vol) with 100 nM ADH1 from *Saccharomyces cerevisiae* digest standard (Waters Corporation, Milford, MA) prior to separation by reversed-phase chromatography and analysis by data-independent (MS^E) label-free mass spectrometry as described before (65) on a Synapt-G2 quadrupole time of flight mass spectrometer (Waters Corporation, Milford, MA). Continuum liquid chromatography (LC)-MS^E data were processed and searched using ProteinLynx GlobalSERVER version 2.5 (PLGS 2.5; Waters Corporation, Milford, MA). Parameter settings were as described in reference 65. Protein identifications were obtained by searching an *N. meningitidis* database (UniProt release 2012_03) with common protein contaminants, as well as ADH1 from *S. cerevisiae* as an internal standard, appended, to address technical variation and allow concentration determinations between different samples (65). The estimation of the false-positive identification rates was performed by searching a randomized version of the abovementioned *N. meningitidis* protein database generated within PLGS 2.5. Data were exported as csv-files for further, detailed analysis. Stringent criteria were applied for quantitation: protein identifications were considered significant only if reported in at least 2 out of 4 biological replicates. Protein false-positive identification rates estimated using this criterion were ~2.3% for a total of 533 identifications. To obtain quantitative information on protein expression in comparing Δ*nmsR*$_A$ Δ*nmsR*$_B$ and wt strains, the amounts in femtomoles estimated by PLGS 2.5 through HI3 peptide quantitation (65) were first normalized by the

sum of all proteins quantified for each individual sample. Subsequently, the average of the normalized femtomoles from the 4 biological replicates was calculated if detected in >1 biological replicate and used to calculate the fold change between Δ*nmsR*$_A$ Δ*nmsR*$_B$ and wt strains if a value for both strains was obtained (see Table S1 in the supplemental material). If a change was ≥1.5-fold up- or downregulated, a *t* test was performed to ascertain whether the change in protein expression was significant, i.e., whether it had a *P* value of ≤0.05 following adjustment for multiple testing according to the method of Benjamini and Hochberg (66). Proteins which were detected in only one of the two strains were reported as uniquely detected only if all of the quadruplicate injections of the biological replicates of one strain yielded quantitative data for this protein while the protein was not detected in any injections of the other strain. When a protein was detected in all injections from one strain and also in one of the replicate injections of the other, the value in normalized femtomoles is given for that single detection (i.e., no fold change value), as this would give the impression that the protein was consistently detected in both strains (Table 1).

Accession number(s). The mass spectrometry proteomics data have been deposited in the ProteomeXchange Consortium (http://www.proteomexchange.org) via the PRIDE partner repository (67) with the data set identifier PXD000891.

SUPPLEMENTAL MATERIAL

Supplemental material for this article may be found at https://doi.org/10.1128/mBio.02293-16.

FIG S1, PDF file, 0.1 MB.

TABLE S1, TXT file, 0.2 MB.

TABLE S2, DOC file, 0.04 MB.

TABLE S3, TXT file, 0.02 MB.

ACKNOWLEDGMENTS

We thank R. B. Pouw and M. L. Ferrando for technical assistance. We acknowledge the PRIDE Team for their efforts in making the mass spectrometry data of this paper publicly available.

This publication made use of the PubMLST website (http://pubmlst.org/) developed by Keith Jolley (16) and hosted at the University of Oxford. The development of that website was funded by the Wellcome Trust.

REFERENCES

1. Stephens DS, Greenwood B, Brandtzaeg P. 2007. Epidemic meningitis, meningococcaemia, and Neisseria meningitidis. Lancet 369:2196–2210. https://doi.org/10.1016/S0140-6736(07)61016-2.
2. Coureuil M, Join-Lambert O, Lécuyer H, Bourdoulous S, Marullo S, Nassif X. 2013. Pathogenesis of meningococcemia. Cold Spring Harb Perspect Med 3:a012393. https://doi.org/10.1101/cshperspect.a012393.
3. Dalebroux ZD, Svensson SL, Gaynor EC, Swanson MS. 2010. ppGpp conjures bacterial virulence. Microbiol Mol Biol Rev 74:171–199. https://doi.org/10.1128/MMBR.00046-09.
4. Kanjee U, Ogata K, Houry WA. 2012. Direct binding targets of the stringent response alarmone (p)ppGpp. Mol Microbiol 85:1029–1043. https://doi.org/10.1111/j.1365-2958.2012.08177.x.
5. Potrykus K, Cashel M. 2008. (p)ppGpp: still magical? Annu Rev Microbiol 62:35–51. https://doi.org/10.1146/annurev.micro.62.081307.162903.
6. Cashel M, Gentry DM, Hernandez VJ, Vinella D. 1996. The stringent response, p 1458–1496. *In* Neidhardt FC, Curtiss R, III, Ingraham JL, Lin ECC, Low KB, Magasanik B, Reznikoff WS, Riley M, Schaechter M, Umbarger HE (ed), *Escherichia coli* and *Salmonella*: cellular and molecular biology, 2nd ed. ASM Press, Washington, DC.
7. Gottesman S, Storz G. 2011. Bacterial small RNA regulators: versatile roles and rapidly evolving variations. Cold Spring Harb Perspect Biol 3:a003798. https://doi.org/10.1101/cshperspect.a003798.
8. Yokoyama K, Ishijima SA, Clowney L, Koike H, Aramaki H, Tanaka C, Makino K, Suzuki M. 2006. Feast/famine regulatory proteins (FFRPs): Escherichia coli Lrp, AsnC and related archaeal transcription factors. FEMS Microbiol Rev 30:89–108. https://doi.org/10.1111/j.1574-6976.2005.00005.x.
9. Hoe CH, Raabe CA, Rozhdestvensky TS, Tang TH. 2013. Bacterial sRNAs: regulation in stress. Int J Med Microbiol 303:217–229. https://doi.org/10.1016/j.ijmm.2013.04.002.
10. Lalaouna D, Simoneau-Roy M, Lafontaine D, Massé E. 2013. Regulatory RNAs and target mRNA decay in prokaryotes. Biochim Biophys Acta 1829:742–747. https://doi.org/10.1016/j.bbagrm.2013.02.013.
11. Michaux C, Verneuil N, Hartke A, Giard JC. 2014. Physiological roles of small RNA molecules. Microbiology 160:1007–1019. https://doi.org/10.1099/mic.0.076208-0.
12. Papenfort K, Vogel J. 2014. Small RNA functions in carbon metabolism and virulence of enteric pathogens. Front Cell Infect Microbiol 4:91. https://doi.org/10.3389/fcimb.2014.00091.
13. Vogel J, Luisi BF. 2011. Hfq and its constellation of RNA. Nat Rev Microbiol 9:578–589. https://doi.org/10.1038/nrmicro2615.
14. Sauer E. 2013. Structure and RNA-binding properties of the bacterial LSm protein Hfq. RNA Biol 10:610–618. https://doi.org/10.4161/rna.24201.
15. Huis in 't Veld RA, Willemsen AM, van Kampen AH, Bradley EJ, Baas F, Pannekoek Y, van der Ende A. 2011. Deep sequencing whole transcriptome exploration of the sigmaE regulon in Neisseria meningitidis. PLoS One 6:e29002. https://doi.org/10.1371/journal.pone.0029002.
16. Jolley KA, Maiden MC. 2010. BIGSdb: scalable analysis of bacterial genome variation at the population level. BMC Bioinformatics 11:595. https://doi.org/10.1186/1471-2105-11-595.
17. Tettelin H, Saunders NJ, Heidelberg J, Jeffries AC, Nelson KE, Eisen JA, Ketchum KA, Hood DW, Peden JF, Dodson RJ, Nelson WC, Gwinn ML, DeBoy R, Peterson JD, Hickey EK, Haft DH, Salzberg SL, White O, Fleischmann RD, Dougherty BA, Mason T, Ciecko A, Parksey DS, Blair E, Cittone H, Clark EB, Cotton MD, Utterback TR, Khouri H, Qin H, Vamathevan J, Gill J, Scarlato V, Masignani V, Pizza M, Grandi G, Sun L, Smith HO, Fraser CM, Moxon ER. 2000. Complete genome sequence of Neisseria meningitidis serogroup B strain MC58. Science 287:1809–1815. https://doi.org/10.1126/science.287.5459.1809.
18. Jyssum K, Borchgrevink B, Jyssum S. 1961. Glucose catabolism in Neisseria meningitidis. 1. Glucose oxidation and intermediate reactions of the Embden-Meyerhof pathway. Acta Pathol Microbiol Scand 53:71–83.
19. Tjaden B, Goodwin SS, Opdyke JA, Guillier M, Fu DX, Gottesman S, Storz G. 2006. Target prediction for small, noncoding RNAs in bacteria. Nucleic Acids Res 34:2791–2802. https://doi.org/10.1093/nar/gkl356.
20. Urban JH, Vogel J. 2007. Translational control and target recognition by

Escherichia coli small RNAs in vivo. Nucleic Acids Res 35:1018–1037. https://doi.org/10.1093/nar/gkl1040.
21. Shine J, Dalgarno L. 1974. The 3′-terminal sequence of Escherichia coli 16S ribosomal RNA: complementarity to nonsense triplets and ribosome binding sites. Proc Natl Acad Sci U S A 71:1342–1346. https://doi.org/10.1073/pnas.71.4.1342.
22. Fisher SD, Reger AD, Baum A, Hill SA. 2005. RelA alone appears essential for (p)ppGpp production when Neisseria gonorrhoeae encounters nutritional stress. FEMS Microbiol Lett 248:1–8. https://doi.org/10.1016/j.femsle.2005.05.014.
23. Pannekoek Y, Speijer D, Van der Ende A. 2014. The regulatory small RNAs of Neisseria, p 41–58. *In* Davies JK, Kahler CM (ed), Pathogenic Neisseria: genomics, molecular biology and disease intervention. Caister Academic Press, Poole, United Kingdom.
24. Mellin JR, Goswami S, Grogan S, Tjaden B, Genco CA. 2007. A novel fur- and iron-regulated small RNA, NrrF, is required for indirect fur-mediated regulation of the sdhA and sdhC genes in Neisseria meningitidis. J Bacteriol 189:3686–3694. https://doi.org/10.1128/JB.01890-06.
25. Metruccio MM, Fantappiè L, Serruto D, Muzzi A, Roncarati D, Donati C, Scarlato V, Delany I. 2009. The Hfq-dependent small noncoding RNA NrrF directly mediates fur-dependent positive regulation of succinate dehydrogenase in Neisseria meningitidis. J Bacteriol 191:1330–1342. https://doi.org/10.1128/JB.00849-08.
26. Ducey TF, Jackson L, Orvis J, Dyer DW. 2009. Transcript analysis of nrrF, a Fur repressed sRNA of Neisseria gonorrhoeae. Microb Pathog 46:166–170. https://doi.org/10.1016/j.micpath.2008.12.003.
27. Cahoon LA, Seifert HS. 2013. Transcription of a cis-acting, noncoding, small RNA is required for pilin antigenic variation in Neisseria gonorrhoeae. PLoS Pathog 9:e1003074. https://doi.org/10.1371/journal.ppat.1003074.
28. Fantappiè L, Metruccio MM, Seib KL, Oriente F, Cartocci E, Ferlicca F, Giuliani MM, Scarlato V, Delany I. 2009. The RNA chaperone Hfq is involved in stress response and virulence in Neisseria meningitidis and is a pleiotropic regulator of protein expression. Infect Immun 77:1842–1853. https://doi.org/10.1128/IAI.01216-08.
29. Isabella VM, Clark VL. 2011. Deep sequencing-based analysis of the anaerobic stimulon in Neisseria gonorrhoeae. BMC Genomics 12:51. https://doi.org/10.1186/1471-2164-12-51.
30. Cecchini G, Schröder I, Gunsalus RP, Maklashina E. 2002. Succinate dehydrogenase and fumarate reductase from Escherichia coli. Biochim Biophys Acta 1553:140–157. https://doi.org/10.1016/S0005-2728(01)00238-9.
31. Tzeng YL, Kahler CM, Zhang X, Stephens DS. 2008. MisR/MisS two-component regulon in Neisseria meningitidis. Infect Immun 76:704–716. https://doi.org/10.1128/IAI.01007-07.
32. Catenazzi MC, Jones H, Wallace I, Clifton J, Chong JP, Jackson MA, Macdonald S, Edwards J, Moir JW. 2014. A large genomic island allows Neisseria meningitidis to utilize propionic acid, with implications for colonization of the human nasopharynx. Mol Microbiol 93:346–355. https://doi.org/10.1111/mmi.12664.
33. Balbontín R, Fiorini F, Figueroa-Bossi N, Casadesús J, Bossi L. 2010. Recognition of heptameric seed sequence underlies multi-target regulation by RybB small RNA in Salmonella enterica. Mol Microbiol 78:380–394. https://doi.org/10.1111/j.1365-2958.2010.07342.x.
34. Papenfort K, Bouvier M, Mika F, Sharma CM, Vogel J. 2010. Evidence for an autonomous 5′ target recognition domain in an Hfq-associated small RNA. Proc Natl Acad Sci U S A 107:20435–20440. https://doi.org/10.1073/pnas.1009784107.
35. Lease RA, Cusick ME, Belfort M. 1998. Riboregulation in Escherichia coli: DsrA RNA acts by RNA:RNA interactions at multiple loci. Proc Natl Acad Sci U S A 95:12456–12461. https://doi.org/10.1073/pnas.95.21.12456.
36. Guillier M, Gottesman S. 2008. The 5′ end of two redundant sRNAs is involved in the regulation of multiple targets, including their own regulator. Nucleic Acids Res 36:6781–6794. https://doi.org/10.1093/nar/gkn742.
37. Pfeiffer V, Papenfort K, Lucchini S, Hinton JCD, Vogel J. 2009. Coding sequence targeting by MicC RNA reveals bacterial mRNA silencing downstream of translational initiation. Nat Struct Mol Biol 16:840–846. https://doi.org/10.1038/nsmb.1631.
38. Shao Y, Feng L, Rutherford ST, Papenfort K, Bassler BL. 2013. Functional determinants of the quorum-sensing non-coding RNAs and their roles in target regulation. EMBO J 32:2158–2171. https://doi.org/10.1038/emboj.2013.155.
39. Sharma CM, Darfeuille F, Plantinga TH, Vogel J. 2007. A small RNA regulates multiple ABC transporter mRNAs by targeting C/A-rich elements inside and upstream of ribosome-binding sites. Genes Dev 21:2804–2817. https://doi.org/10.1101/gad.447207.
40. Beisel CL, Storz G. 2011. The base-pairing RNA spot 42 participates in a multioutput feedforward loop to help enact catabolite repression in Escherichia coli. Mol Cell 41:286–297. https://doi.org/10.1016/j.molcel.2010.12.027.
41. Durand S, Storz G. 2010. Reprogramming of anaerobic metabolism by the FnrS small RNA. Mol Microbiol 75:1215–1231. https://doi.org/10.1111/j.1365-2958.2010.07044.x.
42. Waters LS, Storz G. 2009. Regulatory RNAs in bacteria. Cell 136:615–628. https://doi.org/10.1016/j.cell.2009.01.043.
43. Rehmsmeier M, Steffen P, Hochsmann M, Giegerich R. 2004. Fast and effective prediction of microRNA/target duplexes. RNA 10:1507–1517. https://doi.org/10.1261/rna.5248604.
44. Sievers S, Lund A, Menendez-Gil P, Nielsen A, Storm Mollerup M, Lambert Nielsen S, Buch Larsson P, Borch-Jensen J, Johansson J, Kallipolitis BH. 2015. The multicopy sRNA LhrC controls expression of the oligopeptide-binding protein OppA in Listeria monocytogenes. RNA Biol 12:985–997. https://doi.org/10.1080/15476286.2015.1071011.
45. Mollerup MS, Ross JA, Helfer AC, Meistrup K, Romby P, Kallipolitis BH. 2016. Two novel members of the LhrC family of small RNAs in Listeria monocytogenes with overlapping regulatory functions but distinctive expression profiles. RNA Biol 13:895–915. https://doi.org/10.1080/15476286.2016.1208332.
46. De Lay N, Schu DJ, Gottesman S. 2013. Bacterial small RNA-based negative regulation: Hfq and its accomplices. J Biol Chem 288:7996–8003. https://doi.org/10.1074/jbc.R112.441386.
47. Pannekoek Y, Huis in 't Veld R, Hopman CT, Langerak AA, Speijer D, van der Ende A. 2009. Molecular characterization and identification of proteins regulated by Hfq in Neisseria meningitidis. FEMS Microbiol Lett 294:216–224. https://doi.org/10.1111/j.1574-6968.2009.01568.x.
48. Ishikawa H, Otaka H, Maki K, Morita T, Aiba H. 2012. The functional Hfq-binding module of bacterial sRNAs consists of a double or single hairpin preceded by a U-rich sequence and followed by a 3′ poly(U) tail. RNA 18:1062–1074. https://doi.org/10.1261/rna.031575.111.
49. Otaka H, Ishikawa H, Morita T, Aiba H. 2011. PolyU tail of rho-independent terminator of bacterial small RNAs is essential for Hfq action. Proc Natl Acad Sci U S A 108:13059–13064. https://doi.org/10.1073/pnas.1107050108.
50. Caswell CC, Oglesby-Sherrouse AG, Murphy ER. 2014. Sibling rivalry: related bacterial small RNAs and their redundant and non-redundant roles. Front Cell Infect Microbiol 4:151. https://doi.org/10.3389/fcimb.2014.00151.
51. Lenz DH, Mok KC, Lilley BN, Kulkarni RV, Wingreen NS, Bassler BL. 2004. The small RNA chaperone Hfq and multiple small RNAs control quorum sensing in Vibrio harveyi and Vibrio cholerae. Cell 118:69–82. https://doi.org/10.1016/j.cell.2004.06.009.
52. Svenningsen SL, Tu KC, Bassler BL. 2009. Gene dosage compensation calibrates four regulatory RNAs to control Vibrio cholerae quorum sensing. EMBO J 28:429–439. https://doi.org/10.1038/emboj.2008.300.
53. Tu KC, Bassler BL. 2007. Multiple small RNAs act additively to integrate sensory information and control quorum sensing in Vibrio harveyi. Genes Dev 21:221–233. https://doi.org/10.1101/gad.1502407.
54. Dombroski AJ, Walter WA, Record MT, Jr, Siegele DA, Gross CA. 1992. Polypeptides containing highly conserved regions of transcription initiation factor sigma 70 exhibit specificity of binding to promoter DNA. Cell 70:501–512. https://doi.org/10.1016/0092-8674(92)90174-B.
55. Campbell EA, Muzzin O, Chlenov M, Sun JL, Olson CA, Weinman O, Trester-Zedlitz ML, Darst SA. 2002. Structure of the bacterial RNA polymerase promoter specificity sigma subunit. Mol Cell 9:527–539. https://doi.org/10.1016/S1097-2765(02)00470-7.
56. Murakami KS, Masuda S, Campbell EA, Muzzin O, Darst SA. 2002. Structural basis of transcription initiation: an RNA polymerase holoenzyme-DNA complex. Science 296:1285–1290. https://doi.org/10.1126/science.1069595.
57. Vanderpool CK, Gottesman S. 2004. Involvement of a novel transcriptional activator and small RNA in post-transcriptional regulation of the glucose phosphoenolpyruvate phosphotransferase system. Mol Microbiol 54:1076–1089. https://doi.org/10.1111/j.1365-2958.2004.04348.x.
58. Landgraf JR, Wu J, Calvo JM. 1996. Effects of nutrition and growth rate on Lrp levels in Escherichia coli. J Bacteriol 178:6930–6936. https://doi.org/10.1128/jb.178.23.6930-6936.1996.
59. Piet JR, Huis in 't Veld RA, van Schaik BD, van Kampen AH, Baas F, van

de Beek D, Pannekoek Y, van der Ende A. 2011. Genome sequence of Neisseria meningitidis serogroup B strain H44/76. J Bacteriol 193: 2371–2372. https://doi.org/10.1128/JB.01331-10.
60. Pannekoek Y, van der Ende A. 2012. Neisseria meningitidis. Methods Mol Biol 799:73–89. https://doi.org/10.1007/978-1-61779-346-2_5.
61. van der Ley P, van der Biezen J, Hohenstein P, Peeters C, Poolman JT. 1993. Use of transformation to construct antigenic hybrids of the class 1 outer membrane protein in Neisseria meningitidis. Infect Immun 61: 4217–4224.
62. Hopman CT, Speijer D, van der Ende A, Pannekoek Y. 2010. Identification of a novel anti-sigmaE factor in Neisseria meningitidis. BMC Microbiol 10:164. https://doi.org/10.1186/1471-2180-10-164.
63. Lee DJ, Bingle LE, Heurlier K, Pallen MJ, Penn CW, Busby SJ, Hobman JL. 2009. Gene doctoring: a method for recombineering in laboratory and pathogenic Escherichia coli strains. BMC Microbiol 9:252. https://doi.org/10.1186/1471-2180-9-252.
64. Ruijter JM, Pfaffl MW, Zhao S, Spiess AN, Boggy G, Blom J, Rutledge RG, Sisti D, Lievens A, De Preter K, Derveaux S, Hellemans J, Vandesompele J. 2013. Evaluation of qPCR curve analysis methods for reliable biomarker discovery: bias, resolution, precision, and implications. Methods 59:32–46. https://doi.org/10.1016/j.ymeth.2012.08.011.
65. Kramer G, Woolerton Y, van Straalen JP, Vissers JP, Dekker N, Langridge JI, Beynon RJ, Speijer D, Sturk A, Aerts JM. 2015. Accuracy and reproducibility in quantification of plasma protein concentrations by mass spectrometry without the use of isotopic standards. PLoS One 10: e0140097. https://doi.org/10.1371/journal.pone.0140097.
66. Benjamini Y, Hochberg Y. 1995. Controlling the false discovery rate—a practical and powerful approach to multiple testing. J R Stat Soc Series B Methodol 57:289–300.
67. Vizcaíno JA, Côté RG, Csordas A, Dianes JA, Fabregat A, Foster JM, Griss J, Alpi E, Birim M, Contell J, O'Kelly G, Schoenegger A, Ovelleiro D, Pérez-Riverol Y, Reisinger F, Ríos D, Wang R, Hermjakob H. 2013. The proteomics IDEntifications (PRIDE) database and associated tools: status in 2013. Nucleic Acids Res 41:D1063–D1069. https://doi.org/10.1093/nar/gks1262.
68. Zuker M. 2003. Mfold web server for nucleic acid folding and hybridization prediction. Nucleic Acids Res 31:3406–3415. https://doi.org/10.1093/nar/gkg595.